Hypercrosslinked porous poly(styrene-co-divinylbenzene) resin: a promising nanostructure-incubator for hydrogen storage

Ziwei Tang, Shaofeng Li, Weina Yang, and Xuebin Yu*

Department of Materials Science, Fudan University, Shanghai 200433, China

E-mail: yuxuebin@fudan.edu.cn

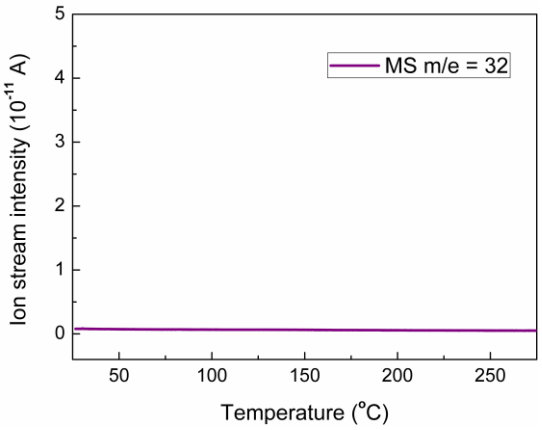

Fig. S1 Mass spectra (m/e = 32) of the PSDB-AB (CH_3OH) with a heating rate of 5 °C·min^{-1}.

From the observation of this MS result, it is revealed that the methanol was moved out from the PSDB-AB (CH_3OH) completely during the vacuum process, thus, it could not contribute to the mass loss and endothermic reaction as indicated in DSC measurement (Fig. 8).

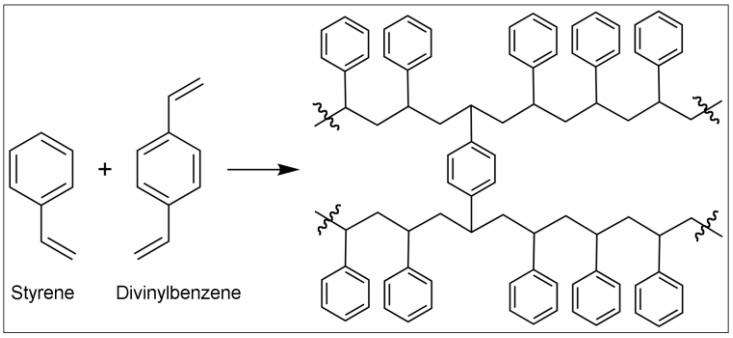

Fig. S2 Reaction scheme for the synthesis of the poly(styrene-co-divinylbenzene).

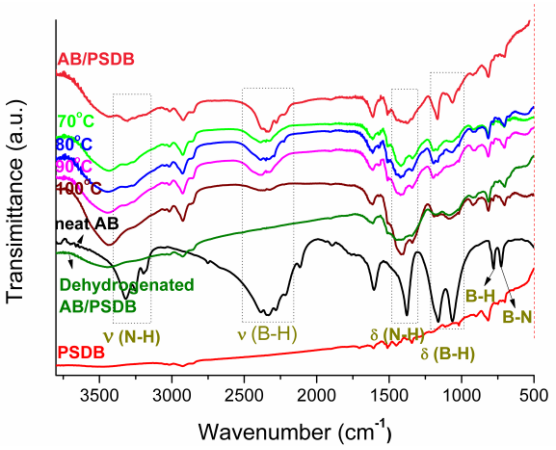

(a)

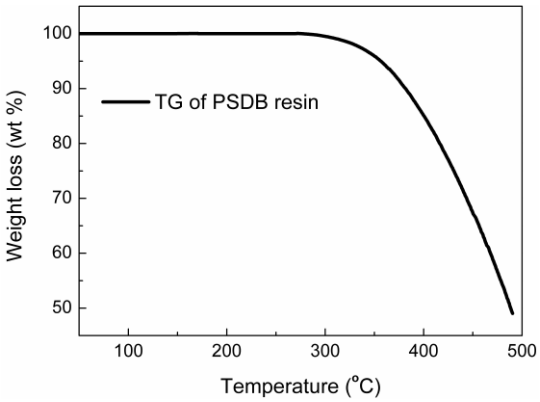

(b)

Fig. S3 (a) FTIR results for the PSDB resin, commercial AB and PSDB-confined AB. (b) TG profile for the PSDB resin with a heating rate 5 °C·min^{-1}.

Fig. S3a shows that the IR spectrum of PSDB-confined AB only couples peaks for both AB and PSDB resin and except for intensity, no obvious wavenumber changes in the B-H, N-H and B-N stretches of AB in PSDB-confined sample with heating treatment to 250 ^{o}C, suggesting that no interaction exists between AB and this supporter. In Fig. S3b, the weight loss from the PSDB resin is observed until heated to 300 ^{o}C, which indicates that no gas liberation, weight loss and structural destruction occurs in the polymer during the measured temperature ranges. Moreover, the large BET surface area (757 m^2·g^{-1}), Langmuir surface area (969 m^2·g^{-1}) and total pore volume (0.88 cm^3·g^{-1}), and low average pore diameter (4.6443 nm). The results above all demonstrate that the hypercrosslinked porous PSDB resin is a potential nanoscaffold with largely available loading areas, chemical inactivity and high thermal stability.

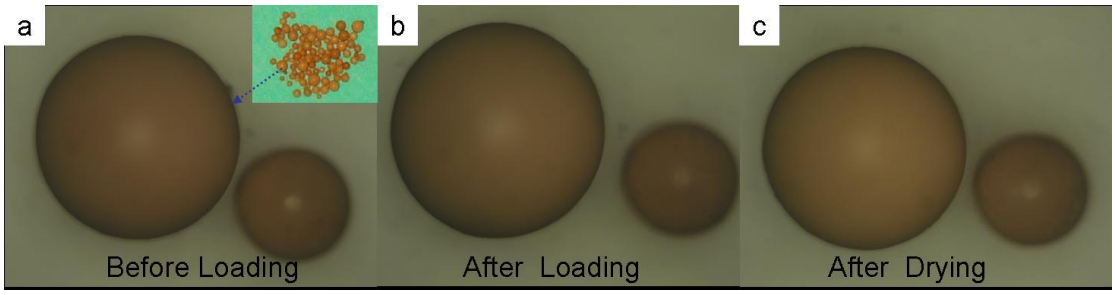

Fig. S4 Microscopic photographs of a bead of the PSDB resin (a) before (the inset image is the photograph of the pristine PSDB resin) and (b) after AB/methanol solution loaded, and (c) after solvent dried.

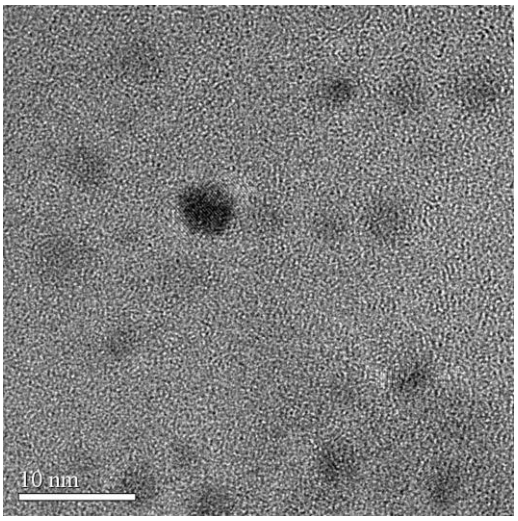

(a)

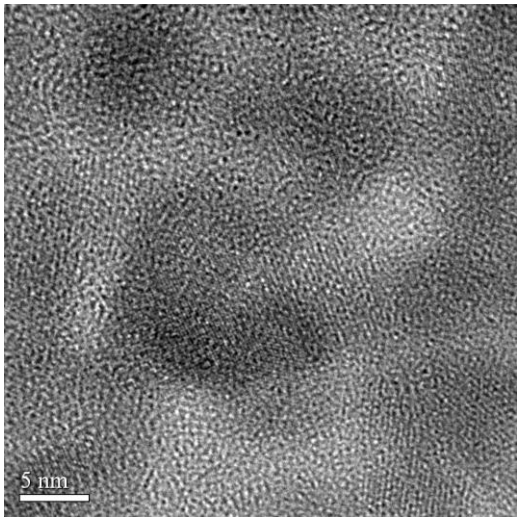

(b)

Fig. S5 HRTEM micrographs (a and b) obtained from the regions shown in Fig. 2e and 2f, respectively.

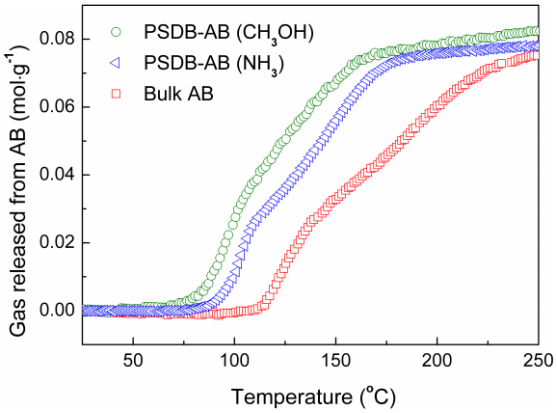

Fig. S6 TPD results of hydrogen released from bulk AB, PSDB-AB (CH_3OH) and PSDB-AB (NH_3), with a heating rate of 5 °C·min^{-1} (The PSDB was not considered as active component in the measurements).

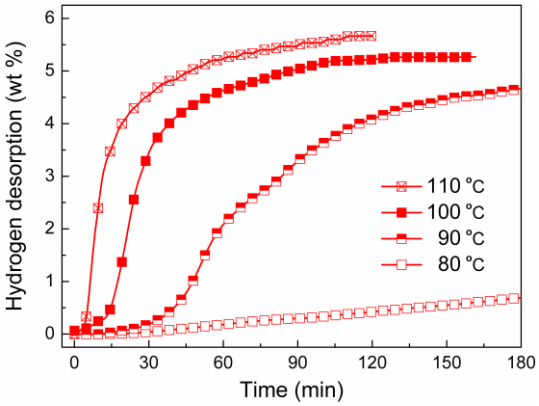

Fig. S7 Isothermal TPD results of hydrogen released from the commercial AB at 80 °C, 90 °C, 100 °C and 110°C.

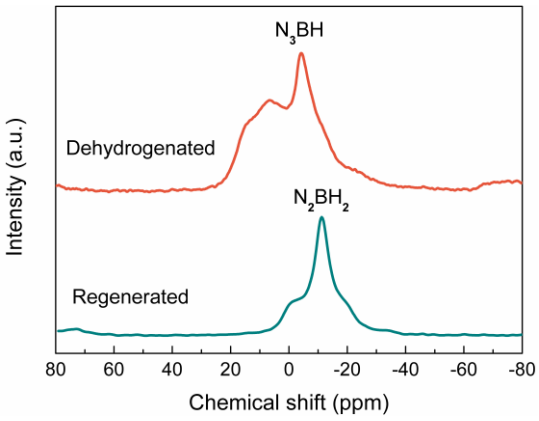

(a)

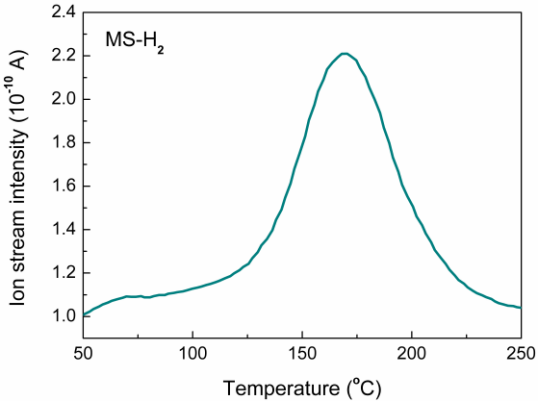

(b)

Fig. S8 (a) ^{11}B NMR of the PSDB-AB (CH_3OH) after dehydrogenation and regeneration process. (b) Mass spectra (m/e = 2) of the regenerated PSDB-AB (CH_3OH) with a heating rate of 5 °C·min^{-1}.

In Fig. S8a, the dehydrogenated products of PSDB-AB (CH_3OH) upon heated at 150 °C for 60 min (> 2 equiv H_2 was released) show a low-unsaturated boron structural feature of $BH(N_3)$, further suggesting its linear growth mechanism. After reduction, the products exhibit a more hydrogen attached to sp^3 type boron, indicating that the regeneration process covert the decomposed products to be an intermediate rather than the starting AB. Fig. S8b further confirms this reduction process, in which a hydrogen evolution peak centered at 170 °C that is neither attributed to the confined AB nor dehydrogenated products is observed.